

P.W. Chan *
Hong Kong Observatory, Hong Kong, China

1. INTRODUCTION

Turbulent airflow occurs at the Hong Kong International Airport (HKIA) when strong winds from east through southwest climb over the mountainous Lantau Island to the south of the airport. Studies have been carried out to measure turbulence intensity using wind profilers (Chan and Chan 2004) and Doppler LIDAR (Chan 2006) for improving the detection of low-level turbulence to be encountered by the aircraft (below 1600 feet or 500 m). This study aims at examining the feasibility of forecasting terrain-induced turbulence using super-high-resolution numerical simulations at a spatial scale less than 100 m (i.e. at the large eddy simulation regime).

Following the practice of the International Civil Aviation Organization (ICAO), turbulence intensity is expressed in terms of the cube root of the eddy dissipation rate (EDR). For low-level turbulence, $EDR^{1/3}$ varying between 0.3 and 0.5 $m^{2/3}s^{-1}$ is taken to be moderate turbulence and $EDR^{1/3}$ of 0.5 $m^{2/3}s^{-1}$ or above refers to severe turbulence.

This paper is organized as follows. Section 2 gives an overview of the numerical model and the computation of turbulence intensity. Section 3 provides the simulation results of two typical cases of terrain-disrupted airflow at HKIA, namely, easterly wind in a stable boundary layer in spring-time and southeasterly flow associated with a tropical cyclone. The forecast distribution of turbulence intensity is compared with actual observations. Conclusions of this study are drawn in Section 4.

2. NUMERICAL MODEL

The Regional Atmospheric Modelling System (RAMS) (Cotton et al. 2003) version 4.4 is used in this study. It is nested with the operational Regional Spectral Model of the Hong Kong Observatory, which has a horizontal resolution of 20 km (Yeung et al. 2005).

Four nesting runs are performed with RAMS using the following horizontal resolutions: 4 km, 800 m, 200 m and 50 m (known as grid 1 to 4 respectively). The model domains of the first three runs are similar to those in Szeto and Chan (2006). The innermost domain (Figure 1b) focuses on the area to the west of HKIA, which is downwind of the mountains (such as Nei Lak Shan, Figure 1a) on Lantau Island in east and southeasterly flow.

In grids 1 and 2, Mellor-Yamada 2.5-level closure scheme (Mellor and Yamada 1982) is used. For grids 3 and 4, Deardorff (1980) scheme is

employed. It is applied to both vertical and horizontal mixing, so that turbulence is isotropic and the diffusion coefficients are the same in all directions. The prognostic turbulent kinetic energy (TKE) equation is solved. The dissipation term in the TKE equation, viz. the EDR (ε), is given by:

$$\varepsilon = \frac{C_D E^{3/2}}{l}$$

where l is a subgrid-scale mixing length which depends on the atmospheric stability (see Deardorff (1980) for details), E the TKE and $C_D = 0.19 + 0.51 / (\Delta x \Delta y \Delta z)^{1/3}$ (Δx is the grid size in the x-direction, etc.).

3. SIMULATION RESULTS

3.1 SPRING-TIME EASTERLY WIND CASE

A fresh to strong easterly airstream affected the coast of southern China on 1 February 2006. LIDAR's velocity imagery (Figure 1a) showed the prevalence of easterly wind in the vicinity of HKIA, apart from an area of reversed flow (coloured in green, i.e. blowing towards the LIDAR) along the northwestern coast of Lantau Island as a result of terrain disruption. These features are reproduced well in the 4-hour simulation results (Figure 1b) of the RAMS run initialized at 18 UTC, 1 February.

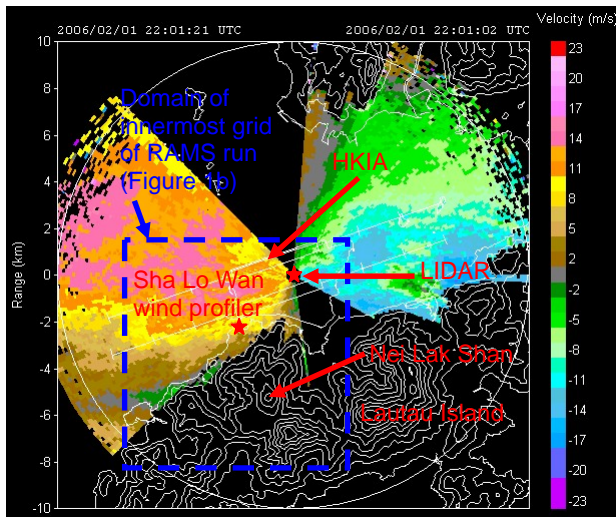
Following the method described in Chan (2006), the EDR map is calculated from LIDAR radial velocity (Figure 1c). It reveals that:

- (i) moderate to severe turbulence (yellow and red) occurred to the southwest of HKIA, along the foot of Nei Lak Shan – region (i);
- (ii) moderate turbulence (green) appeared to the west of HKIA – region (ii).

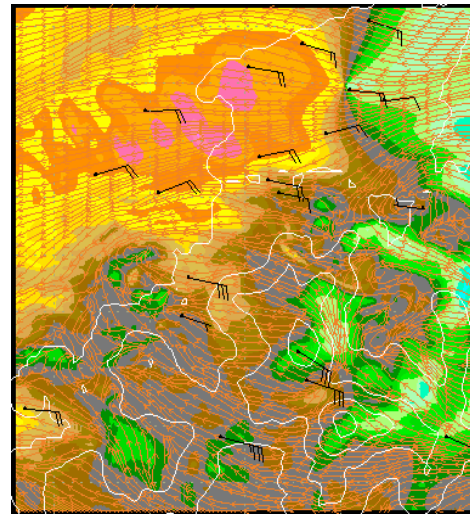
Model simulation (Figure 1d) gives a similar distribution of turbulence intensity. The airflow was the most turbulent in region (i) because of the proximity to the mountainous terrain. The easterly jet and the terrain effect produced moderate turbulence in region (ii). Difference between LIDAR-measured and simulated EDR values is observed at about 10 km southwest of HKIA. This is due to the much higher altitude of the laser beam at that region (about 225 m AMSL) in 1-degree conical scan compared to 50 m AMSL in the model simulation results.

Model results are also compared with the EDR measurements by the wind profiler at Sha Lo Wan (see Figure 1a for location). The vertical variations of $\varepsilon^{1/3}$ in the wind profiler observations (Figure 2a) and simulation (Figure 2b) are similar. In general, $\varepsilon^{1/3}$ decreased with altitude and was less than 0.2 $m^{2/3}s^{-1}$ starting from around 400 m above ground. However,

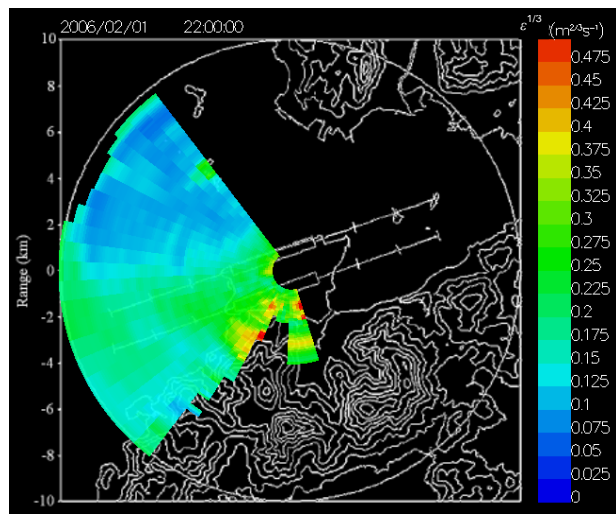
* Corresponding author address: P.W. Chan, Hong Kong Observatory, 134A Nathan Road, Hong Kong email: pwchan@hko.gov.hk



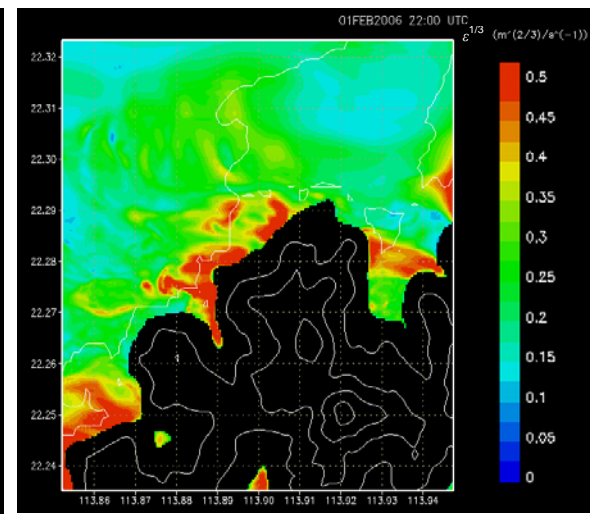
(a)



(b)

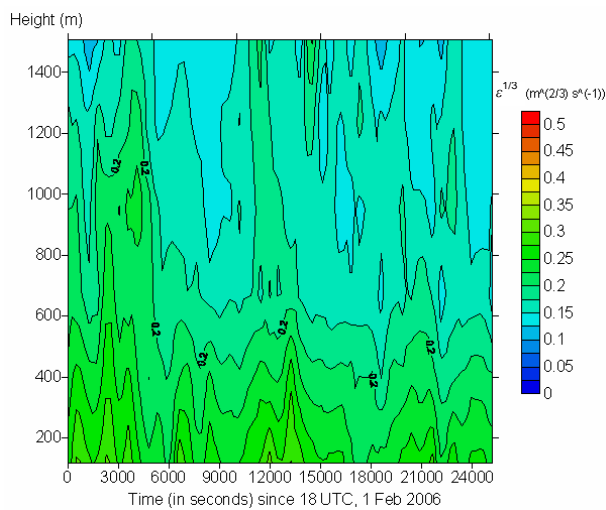


(c)

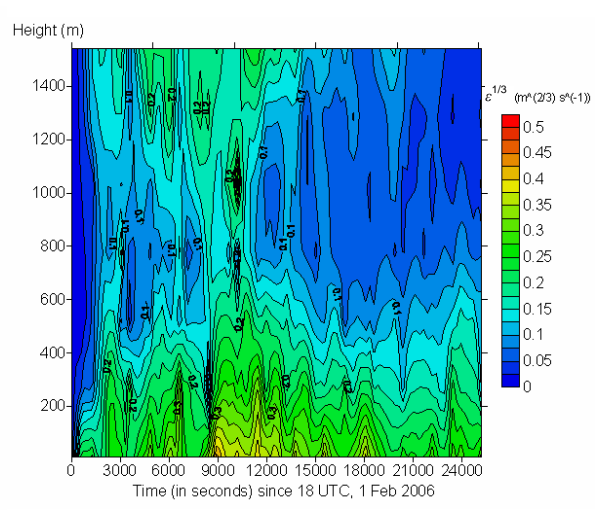


(d)

Figure 1 LIDAR's radial velocity imagery from 1-degree conical scan at 22 UTC, 1 February 2006 (a) and the corresponding EDR map (c). The corresponding RAMS simulation results (the forecast initialized at 18 UTC) at 50 m AMSL are given in (b) and (d) respectively. The wind barbs in (b) are the model simulated winds at 10 m AMSL at selected locations and the brown lines are the streamlines at 50 m AMSL. The radial velocity scale in (b) is the same as in (a).



(a)



(b)

Figure 2 Vertical variation of turbulence intensity as measured by Sha Lo Wan wind profiler (a) and the model results at that location (b). Data in (a) start at the first gate of the profiler (about 120 m AMSL).

the rate of decrease was not a constant and sometimes EDR fell less rapidly with height. For instance, as measured by the wind profiler, $\epsilon^{1/3}$ was larger than $0.175 \text{ m}^{2/3}\text{s}^{-1}$ all the way up to 1.5 km above ground (coloured light green in Figure 2a) between 11000 and 13000 seconds from 18 UTC, 1 February. A similar episode was also forecast in the model, though at an earlier time (between 10000 and 11000 seconds, Figure 2b).

The major discrepancies between the profiler measurements and the model results are: (a) the model tends to give larger $\epsilon^{1/3}$ near ground, exceeding $0.3 \text{ m}^{2/3}\text{s}^{-1}$ which is not observed in reality, and (b) $\epsilon^{1/3}$ in general drops more rapidly with height in the simulation. Fast and Shaw (2002) reported similar discrepancies in the RAMS simulations for Vertical Transport and Mixing (VTMX) campaign at Salt Lake Valley, U.S.A. using Mellor-Yamada 2.5-level closure scheme. They conjectured that the differences might be due to over-prediction of vertical mixing near the ground and under-prediction of TKE aloft in the model simulations. The latter behaviour was also observed in simulations using Deardorff scheme (Trini Castelli et al. 2005). The issues could be studied further when vertical profiles of TKE and mixing length are measured and new turbulence schemes are developed based on the measurements.

In the nesting run of the numerical model at this super-high spatial resolution, one major challenge is the lack of an appropriate turbulence parameterization scheme in the "intermediate" length scale in the order of several hundred metres. The sensitivity of the modelling results to the choice of the turbulence parameterization scheme in this "intermediate" scale is also considered for this spring-time case. Two more nesting runs have been performed:

- (i) Mellor-Yamada scheme for grids 1-3, Deardorff scheme in grid 4;
- (ii) Mellor-Yamada scheme for grids 1-2, local scheme of Smagorinsky in RAMS (without the use of TKE equation) in grid 3, and Deardorff scheme in grid 4.

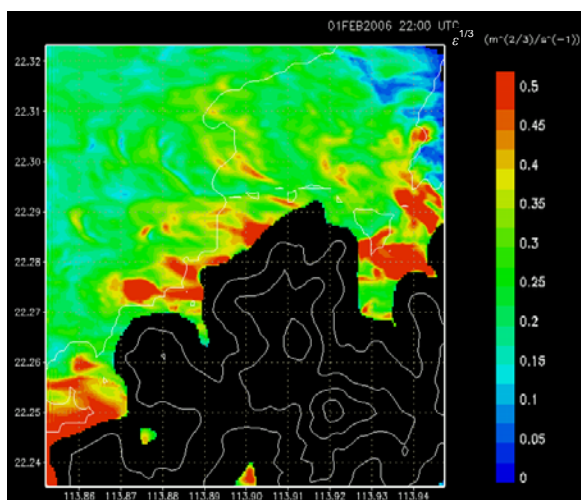


Figure 3 Turbulence intensity field obtained in the RAMS run with Smagorinsky turbulence parameterization scheme in grid 3.

The modelled wind and turbulence intensity fields from the three simulations are largely similar (e.g. the $\epsilon^{1/3}$ field based on the nesting run (ii) in Figure 3, c.f. Figure 1d). The simulation results do not seem to be very sensitive to the choice of turbulence parameterization scheme in the intermediate grid.

3.2 TYPHOON CASE

Typhoon Imbudo case on 24 July 2003 is considered here. This was the day with the largest number of severe turbulence reports from aircraft since the opening of HKIA in 1998.

Imbudo brought gale-force southeasterly wind to the airport area. The LIDAR's radial velocity imagery (Figure 4a) is similar to the result of RAMS simulation initialized at 00 UTC of 24 July (Figure 4b) except that the blobs of reversed flow (coloured green in Figure 4a) to the west of HKIA extended further downstream of Lantau Island in reality. Because of the much stronger background wind, the turbulence intensity (Figure 4c) was generally higher in this event compared to the spring-time case. There were streaks of severe turbulence (coloured red in Figure 4c) extending for about 4 km from the mountains on Lantau Island. This feature is well captured in the model prediction (Figure 4d).

The model-simulated turbulence intensity has about the same magnitude as the measurement from the wind profiler in the first couple of hundred metres above ground (Figure 5). Further aloft, it again decreases too rapidly with height when compared to actual observations. Nonetheless, it is interesting to note that the model simulated results suggest that moderate to severe turbulence can penetrate to a height of about 1000 m, similar to the wind profiler observations.

4. CONCLUSIONS

The RAMS model runs at a horizontal resolution below a couple of hundred metres (the regime of large eddy simulation) are found to reproduce successfully the salient features of the spatial distribution of turbulence intensity in two typical episodes of terrain-disrupted airflow at HKIA. The forecast $\epsilon^{1/3}$ field in the first several hundred metres above ground compares well with the actual observations and has potential for predicting low-level turbulence in aviation applications. The major problem with the simulation result is that the turbulence intensity in general decreases too fast with altitude compared to the actual observations. It is more pronounced in the tropical cyclone case. The issue would be addressed in future studies.

Acknowledgement

The author would like to thank Mr. Keiya Yumimoto of Kyushu University for useful discussions.

References

Chan, P.W., and S.T. Chan, 2004: Performance of eddy dissipation rate estimates from wind profilers in turbulence detection. *11th Conference on Aviation, Range, and Aerospace*

- Meteorology*, American Meteorological Society, Massachusetts, U.S.A.
- Chan, P.W., 2006: Generation of eddy dissipation rate map at the Hong Kong International Airport based on Doppler LIDAR data. *12th Conference on Aviation, Range, and Aerospace Meteorology*, American Meteorological Society, Georgia, U.S.A.
- Cotton, W.R. et al., 2003: RAMS 2001: Current status and future directions. *Meteor. Atmos. Phys.*, **82**, 5-29.
- Deardorff, J.W., 1980: Stratocumulus-capped mixed layers derived from a three-dimensional model. *Bound.-Layer Meteor.*, **18**, 495–527.
- Fast., J.D., and W.J. Shaw, 2002: An evaluation of mesoscale model predictions of turbulence kinetic energy and dissipation. VTMX Science Meeting, Salt Lake City, U.S.A. (<http://www.pnl.gov/vtmx/presentations2002.html>)
- Mellor, G. L., and T. Yamada, 1982: Development of a turbulence closure model for geophysical fluid problems. *Rev. Geophys. Space Phys.*, **20**, 851–875.
- Szeto, K.C., and P.W. Chan, 2006: High resolution numerical modelling of windshear episodes at the Hong Kong International Airport. *12th Conference on Aviation, Range, and Aerospace Meteorology*, American Meteorological Society, Georgia, U.S.A.
- Trini Castelli, S., E. Ferrero, D. Anfossi, and R. Ohba, 2005: Turbulence closure models and their application in RAMS. *Environmental Fluid Mechanics*, **5**, 169–192.
- Yeung, L.H.Y., P.K.Y. Chan and E.S.T. Lai, 2005: Impact of radar rainfall data assimilation on short-range quantitative precipitation forecasts using four-dimensional variational analysis technique. *32nd Conference on Radar Meteorology*, American Meteorological Society, New Mexico (on-line proceedings).

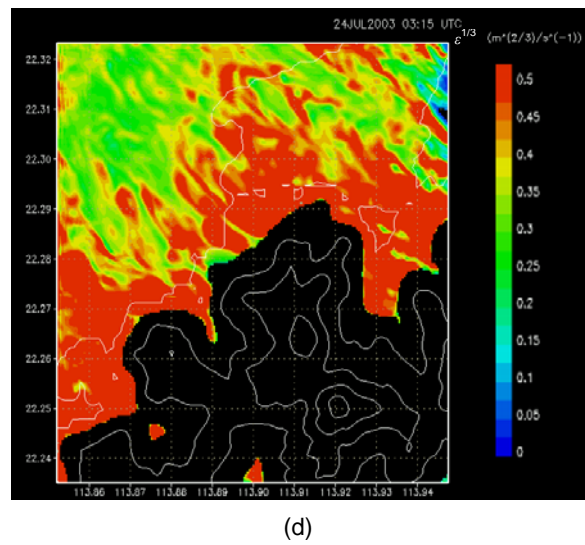
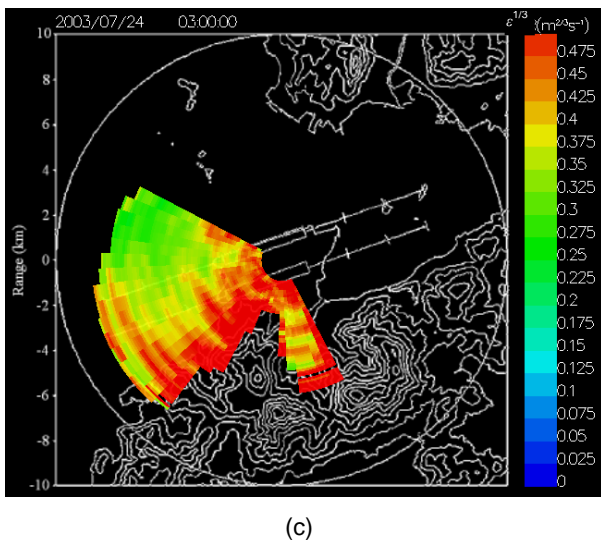
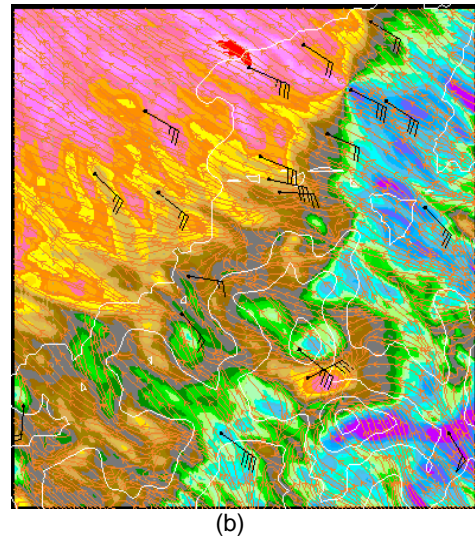
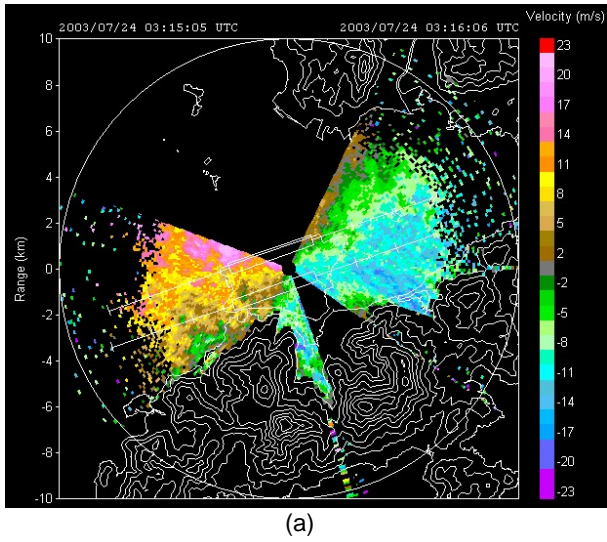


Figure 4 Same as Figure 1, but for typhoon Imbudo case on 24 July 2003.

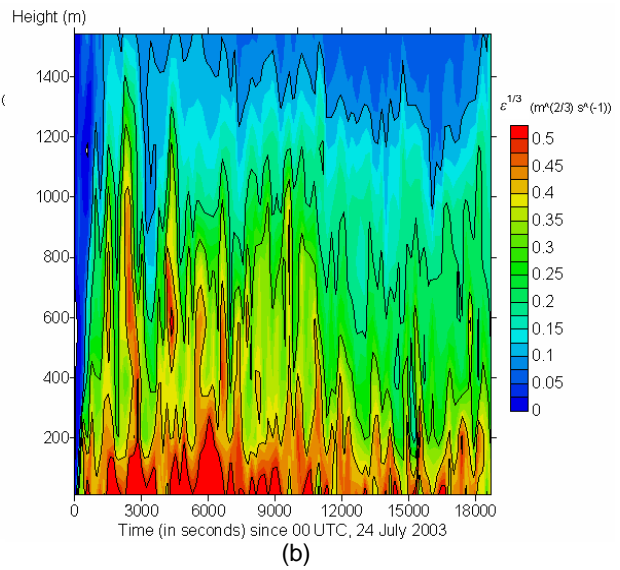
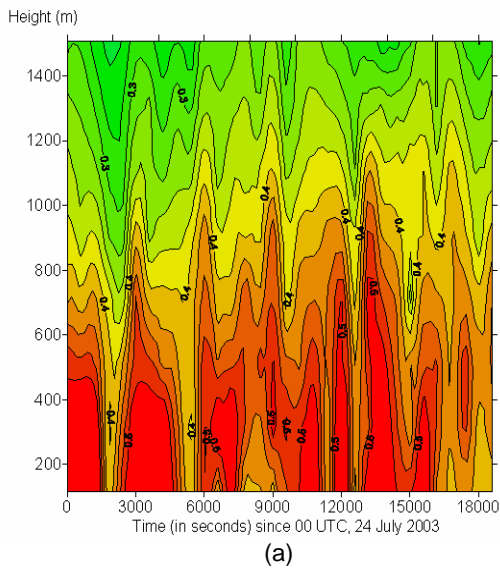


Figure 5 Same as Figure 2, but for typhoon Imbudo case.